Front. Environ. Sci. Eng. 2013, 7(3): 464–473
DOI 10.1007/s11783-012-0430-y

RESEARCH ARTICLE

Removal of elemental mercury with $Mn/Mo/Ru/Al_2O_3$ membrane catalytic system

Yongfu GUO[1,2], Naiqiang YAN (✉)[1], Ping LIU[1], Shijian YANG[1], Juan WANG[1], Zan QU[1]

1 School of Environmental Science and Engineering, Shanghai Jiao Tong University, Shanghai 200240, China
2 Department of Municipal Engineering, Suzhou University of Science and Technology, Suzhou 215011, China

Abstract In this work, a catalytic membrane using $Mn/Mo/Ru/Al_2O_3$ as the catalyst was employed to remove elemental mercury (Hg^0) from flue gas at low temperature. Compared with traditional catalytic oxidation (TCO) mode, Mn/Al_2O_3 membrane catalytic system had much higher removal efficiency of Hg^0. After the incorporation of Mo and Ru, the production of Cl_2 from the Deacon reaction and the retainability for oxidants over Mn/Al_2O_3 membrane were greatly enhanced. As a result, the oxidization of Hg^0 over Mn/Al_2O_3 membrane was obviously promoted due to incorporation of Mo and Ru. In the presence of 8 ppmv HCl, the removal efficiency of Hg^0 by $Mn/Mo/Ru/Al_2O_3$ membrane reached 95% at 423 K. The influence of NO and SO_2 on Hg^0 removal were insignificant even if 200 ppmv NO and 1000 ppmv SO_2 were used. Moreover, compared with the TCO mode, the $Mn/Mo/Ru/Al_2O_3$ membrane catalytic system could remarkably reduce the demanded amount of oxidants for Hg^0 removal. Therefore, the $Mn/Mo/Ru/Al_2O_3$ membrane catalytic system may be a promising technology for the control of Hg^0 emission.

Keywords flue gas, elemental mercury, membrane, catalysis, transition metal

1 Introduction

Mercury removal from coal-fired flue gas has become a topic with increasing legislative and scientific interest [1]. In coal-derived flue gas, there are three basic forms of mercury: elemental mercury (Hg^0), oxidized mercury (Hg^{2+}) and particle-bound mercury (Hg_p) [2]. Hg_p can be captured by electrostatic precipitators (ESPs) and fabric filters (FFs). Hg^{2+} is soluble in water and readily captured by the wet flue gas desulfurization (WFGD) equipment [2–5]. Hg^0 is volatile and insoluble in water, and thus, it is poorly captured using conventional control technologies [6].

There exist some potential approaches to enhance Hg^0 removal from coal-fired flue gas. Injection of proper oxidants into flue gas is an effective way to enhance the conversion of Hg^0 to Hg^{2+}. Then, the formed Hg^{2+} can be removed by the ESPs or FFs. So far, most of the existing research focuses on the oxidization of elemental mercury at high temperature, especially at > 523 K [7–11]. However, there are some problems in the application of traditional catalytic oxidation technology (TCO), such as the deposition of dust [9] and the poisoning of SO_2 and NO. Therefore, the catalysts may be installed downstream the ESPs or FFs in order to obtain higher efficiency of Hg^0 removal, where the temperature is about 423 K [12].

Some transition metal oxide catalysts, (for example manganese oxide), showed an excellent activity for Hg^0 oxidization at high temperatures [6,9,13]. However, most of them showed a poor activity for Hg^0 oxidization at low temperatures. Furthermore, the presence of SO_2 showed a serious interference with Hg^0 oxidization at low temperatures.

In this work, a unique membrane catalytic system (MCs) with HCl as the oxidant precursor was employed to improve the removal of Hg^0 from flue gas at low temperature. MnO_2/Al_2O_3 was employed as the main catalytic components of the MCs for Hg^0 removal. Then, the transition metals of Mo and/or Ru were introduced into the MnO_2/Al_2O_3 membrane to improve the conversion efficiencies of Hg^0 to Hg^{2+}. Furthermore, the TCO mode using $Mn/Mo/Ru/Al_2O_3$ as the catalyst was studied as a comparison.

2 Experiment

2.1 Experimental assembly

The MCs assembly used for Hg^0 removal is shown in Fig. 1. It consisted of a self-made mercury permeation device

Received October 3, 2011; accepted December 11, 2011

E-mail: nqyan@sjtu.edu.cn

[14,15], a membrane reactor, an online cold vapor atomic adsorption spectrophotometry (CVAAS), a gas preparation system and an activated carbon catcher. The self-made mercury permeation device was immersed in a temperature-controlled oil bath, which was maintained at the demanded temperature (±0.1°C), to provide a stable concentration of gaseous Hg^0 at a given temperature. During the test, the reactor was placed in a temperature-controlled electric furnace (SK2-1-10, Shanghai Yifeng Co. Ltd., China) which maintained the reaction temperature at the desired temperature within a range of 1°C. The activated carbon catcher was used to capture gaseous Hg^0 and mercury compounds in the outlet of the reactor.

The membrane reactor consisted of a quartz tube (360 mm in length with an inner diameter of 16 mm) and a tubular ceramic membrane mounted coaxially. The inlet (C_0) or outlet (C) concentration of Hg^0 was determined online using a CVAAS (SG-921, Jiangfen Ltd., China). The compressed air or N_2 was employed as the carrier gas to transport Hg^0 vapor. If HCl was injected at port 1, the assembly was a typical MCs process. If HCl was injected from port 2, the process can be regarded as the TCO mode.

2.2 Catalyst preparation

The MCs employed a porous ceramic tube (pore diameter of 5 μm, inner diameter of 8 mm, outer diameter of 12 mm, Brunauer–Emmett–Teller (BET) surface of 4.1 $m^2 \cdot g^{-1}$, length of 50 mm. Hefei Great Wall Co. Ltd., China) as the membrane material, which was also used as the carrier of catalysts. The catalysts were prepared by wet impregnation method with the aqueous solution of manganese nitrate (50 wt.%) as a precursor. The amount of manganese oxide loaded on Al_2O_3 was about 8 wt.%. The amounts of Mo and Ru incorporated into MnO_x were about 1.5 wt.% and 1 wt.%, respectively. The catalysts prepared by wet impregnation method were expressed as Mn, Mo, Ru, Mn-Mo, Mn-Ru, and Mn-Mo-Ru catalysts. All chemicals used for the catalyst preparation, including the precursors of $Mn(NO_3)_2$, $(NH_4)_6Mo_7O_{24} \cdot 4H_2O$ and $RuCl_3 \cdot 3H_2O$, were of analytical grade and purchased from Sino-pharm Chemical Reagent Corp., China.

2.3 Performance evaluation

The experiments were performed in the MCs at 423 K with the simulated flue gas containing SO_2, NO and/or HCl. The total flow rate was 25.0 $L \cdot h^{-1}$. The flow rates of SO_2 and NO were all set at 2.0 $L \cdot h^{-1}$ except HCl, which had a flow rate of 1.0 $L \cdot h^{-1}$, and the operation time was 4 h. First, the capacity of catalysts for Hg^0 adsorption was investigated. Then, the removal of Hg^0 was studied in the presence of 8 ppmv HCl. At last, the influence of SO_2 and/or NO over the MCs was also investigated.

2.4 Characterizations

The contents of Mn, Mo, and Ru in the catalysts were quantified by a flame atomic absorption spectrometry (AAS, KLAS-1000CA, Kwicklink Chemical Co., Ltd., UK). The content of Hg on the surface of catalysts was analyzed with an RA-915 Mercury Analyzer (Lumex Ltd., Russia). The BET surface area was determined using a nitrogen adsorption desorption apparatus (ASAP 2010 M + C, Micromeritics Inc., USA). All the samples were degassed at 423 K prior to BET measurements. The X-ray diffractometer (XRD, D/max-2200/PC, Rigaku Corp., Japan) was recorded between 20° and 80° at a step of 5°·min^{-1} operating at 40 kV and 20 mA using Cu Kα radiation. An X-ray photoelectron spectroscopy (XPS,

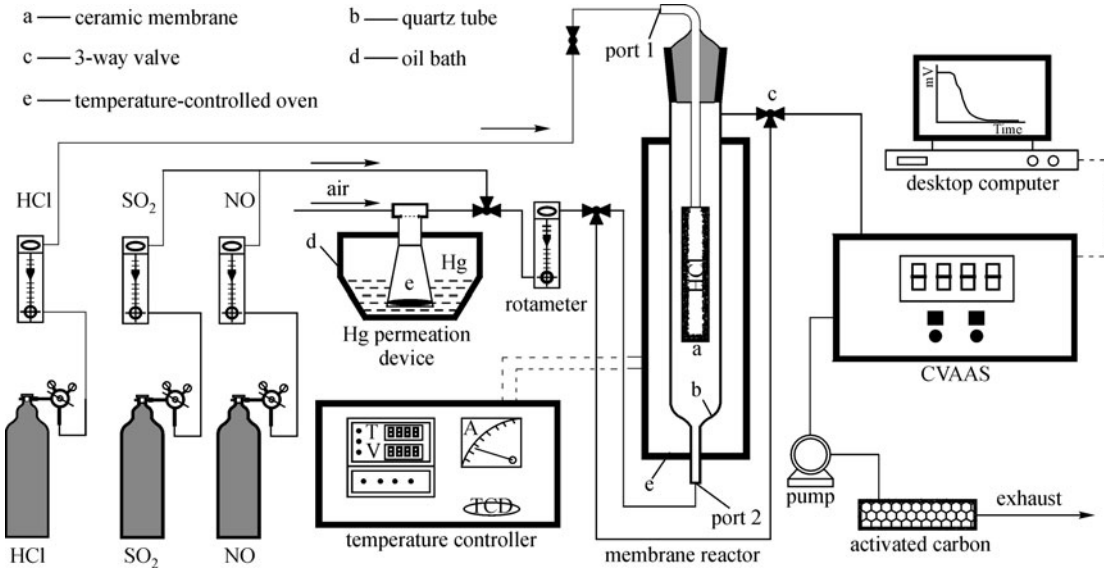

Fig. 1 Experimental scheme of the MCs

PHI-5000C ESCA, PHI Corp., USA) with Mg Kα ($h\nu$ = 1253.6 eV) as the excitation source was used to determine the binding energies (BE) of Mn, Mo, Ru, and Hg. The C 1s peak at 284.6 eV was taken as a reference for the binding energy calibration. The morphology of the catalysts was observed using a field emission scanning electron microscope (FE-SEM, SIRION 200, FEI Corp., USA), operating in backscatter mode at 20 kV accelerating voltage. An energy dispersive X-ray spectrometer (EDX, INCA, OXFORD Corp., UK) was used to examine the distribution of doped metal element on the surface of the catalysts.

Hydrogen temperature programmed reduction (H_2-TPR) was performed on a chemisorption analyzer (TP-5000, Tianjin Xianquan Co. Ltd., China) under a 4.9 vol% H_2/Ar gas flow (30 mL·min^{-1}) at a rate of 10°C·min^{-1} from 150°C to 650°C. Before the test, the samples (50 mg) were firstly pretreated in a flow of 20 vol% O_2/Ar (30 mL·min^{-1}) at 450°C for 30 min to remove water and carbonates from the surface.

2.5 Mass balance analysis

After HCl was used, the speciation of Hg over the MCs mainly included effluent oxidized mercury (Hg^{2+}-out), effluent elemental mercury (Hg^0-out) and adsorbed mercury on the spent catalysts (mainly oxidized mercury, Hg^{2+}-ad). Fresh catalysts after catalytic oxidation at 423 K were used to analyze the speciation of Hg. Meanwhile, Hg sampling and analysis were carried out according to the Ontario Hydro Method (OHM).

The operation of OHM was stated as follows: The Hg^{2+}-out was collected in the first three impingers containing chilled aqueous potassium chloride solution (1 mol·L^{-1} KCl), because the oxidized mercury was water soluble. The Hg^0-out was collected in subsequent four impingers. The first impinger was filled with chilled aqueous acidic solution of hydrogen peroxide (10% (v/v) H_2O_2 and 5% (v/v) HNO_3). The other three impingers were filled with chilled aqueous acidic solutions of potassium permanganate (4% (w/v) $KMnO_4$ and 10% (v/v) H_2SO_4). The Hg^0-out was firstly oxidized into the oxidized mercury and then trapped in the solution. A schematic of the OHM can be found elsewhere [16].

The concentrations of Hg^{2+}-out and Hg^0-out in the effluent gas were recovered, digested and analyzed with the CVAAS. The content of Hg^{2+}-ad was analyzed with the RA-915 Mercury Analyzer. The CVAAS system was made up of a light source, two quartz pipes, a photodiode and a data transition and acquisition device. A low-pressure mercury lamp was used as the 253.7 nm UV light source, which could be absorbed by Hg^0 vapor. Two quartz pipes were oppositely installed at the outlet of the reactor, which allowed the UV beam to pass them efficiently. After the optical assembly, the UV beam was divided into two parts. One was used as the reference and the other as the monitor. As the UV beam passing through the quartz pipe, the variation of the UV beam intensity was detected and converted into the electrical signal by a photodiode. And then the signal was collected with a data transition and acquisition device (N2000, Zhejiang Zhida Co. Ltd., China) and stored in a computer. Thus, the concentration of Hg^0-out was measured in situ, with the capability of a time resolution of 20 ms.

The oxidized mercury contained in the KCl impinger was analyzed using acidic 0.5 mol·L^{-1} Sn(II)-chloride solution as a reducing agent to reduce Hg^{2+} to Hg^0. Subsequently, the mercury-laden solution was purged with a carrier gas (air) into the CVAAS, where the maximum amount of mercury was detected, analyzed and recorded.

3 Results and discussion

3.1 Characterization of catalysts

XRD patterns of synthetic catalysts are shown in Fig. 2. Their characteristic reflections mainly corresponded to the standard card of MnO_2 (JCPDS 24-0735). Meanwhile, the peaks corresponding to Mn_2O_3 can also be observed [17]. Furthermore, the peaks centered at 23.12° and 51.32° were assigned to MoO_3 (JCPDS 47-1081), and the peaks centered at 26.04° and 53.76° were assigned to MoO_2 (JCPDS 50-0739). As shown in Fig. 2(b), the characteristic peaks of the ruthenium at 2θ = 28.01° (hardly shown) and 35.05° (overlapped by the peaks of Al_2O_3) indicated that they were attributed to RuO_2 (JCPDS 40-1290 and 43-1027).

The pore size, the BET surface area (S_{BET}) and surface atom concentrations of the catalysts were tested and listed in Table 1. It shows that both S_{BET} and pore size of the catalysts decreased after the wet impregnation.

3.2 Hg^0 adsorption

The adsorption of Hg^0 on the MCs at 423 K (in the absence of HCl and SO_2) is shown in Fig. 3. Figure 3 shows that Mo catalyst had the worst adsorption ability for Hg^0, and the removal efficiency of Hg^0 over Mn catalyst was only 20%. Furthermore, the removal efficiency of elemental mercury over Mn catalyst obviously increased due to the incorporation of Mo and/or Ru.

Figure 3 also shows that the removal efficiency of elemental mercury by Mn catalyst under N_2 atmosphere (8%) was much less than that under air atmosphere (16%). It indicates that elemental mercury adsorption on Mn catalyst was promoted due to the presence of O_2.

3.3 Performance of Hg^0 conversion

Conversion efficiency of elemental mercury over various transition metals in the presence of 8 ppmv HCl is shown

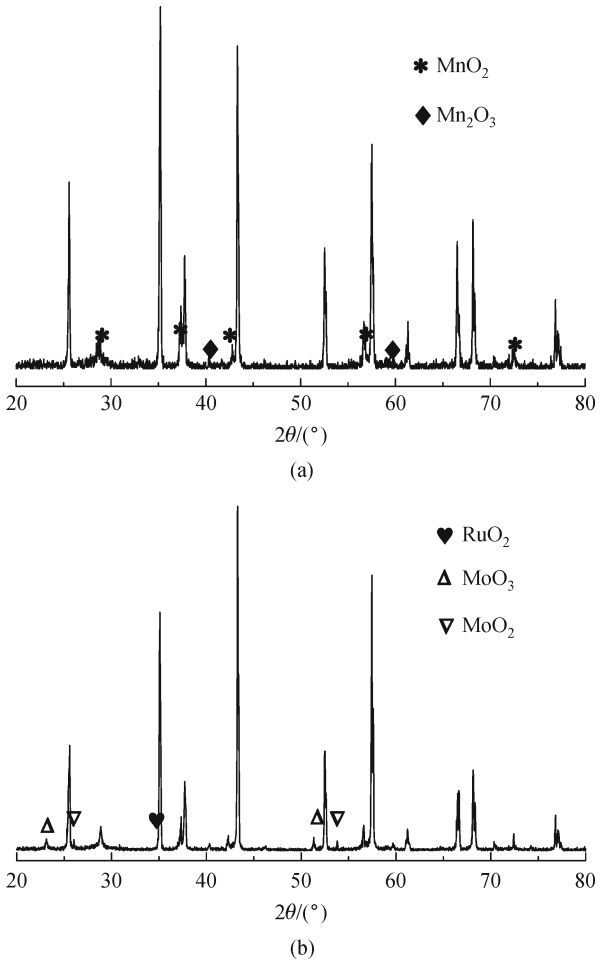

Fig. 2 X-ray diffraction patterns (a) Mn catalyst and (b) Mn-Mo-Ru catalyst

in Fig. 4. It shows that elemental mercury conversion over Mn-Mo-Ru catalyst (conversion efficiency of 61% at 423 K) was much higher than those of others. On the catalysts of Mn, Mn-Mo, Mn-Ru, and Mn-Mo-Ru, mercury (II) chloride accounted for 62.8%, 71.4%, 90.6%, and 93.4%, respectively. It indicates that the ratio of mercury (II) to the removed mercury on Mn catalyst increased after the addition of transition metals, which may results from the promotion of the conversion of HCl to Cl/Cl_2 through the Deacon reaction [7].

According to previous studies, the Deacon reaction was the predominant pathway for Hg^0 oxidation through the combination of Hg^0 and active chlorine ($[Cl]^*$, derived from HCl) in the presence of metal catalysts [18,19]. Although gaseous Cl_2 can react with gaseous Hg^0 in the gas phase to form Hg^{2+}, Cl atom is the active intermediate [7,20]. Namely, Cl atom is a much stronger oxidizing agent over HCl because of the difference of their valence electron configurations. This will result in the difference of affinity for Hg^0 [15,21]. However, it is difficult to determine in situ the yield of atomic chlorine of $[Cl]^*$ produced from the Deacon reaction at test conditions.

To further confirm the effect of the Deacon reaction on Hg^0 conversion and the improvement of transition metals on the Deacon reaction, the test employed 0.5 ppmv Cl_2 as oxidants. Noticeably, the concentration of Cl_2 used is equal to the amount of Cl_2 produced from the Deacon reaction with 8 ppmv HCl. As shown in Fig. 5, the mean efficiencies were below 50% when Cl_2 was used as a substitute for HCl. The result effectively validates the effect of transition metals on the conversion of Hg^0 in the MCs. Compared Fig. 4 with Fig. 5, it is clear that the transition metals played a key role in the conversion of HCl to $[Cl]^*$, and this can be used to partly explain the reasons why the efficiencies were significantly increased with Mn-Mo-Ru catalyst.

3.4 Retainability influence of HCl

Our previous studies demonstrated that the penetration process of HCl in the membrane material had an important effect on the Deacon reaction [3]. To investigate the influence of penetration process of HCl on the conversion of Hg^0 and the activation of HCl, the variation of Hg^0 removal was tested at different injection conditions of oxidants (MCs mode, HCl injected from port 1). Simultaneously, TCO mode (HCl injected from port 2) was conducted as a comparison.

As shown in Fig. 6, the Hg^0 concentration dropped quickly with the injection of HCl, and it became stable within 120 min in the MCs and 300 min in the TCO mode. However, the removal of Hg^0 increased quickly when the injection of HCl was stopped in the TCO mode. Compared curve a with curve b in Fig. 6, it indicates that the

Table 1 Composition and properties of different catalysts

catalysts	S_{BET}/($m^2 \cdot g^{-1}$)	surface atom concentrations obtained by AAS or EDX/%						pore diameter/ μm
		Cl	O	Mn	Mo	Ru	O/Mn	
virgin tube	4.1	–	46.2	–	–	–	–	4.7
Mn	1.4	–	40.8	8.1	–	–	5.0	1.9
Mn-Mo	1.5	–	41.0	8.0	1.75	–	5.1	1.6
Mn-Ru	2.1	NA	41.2	8.1	–	0.9	5.1	1.7
Mn-Mo-Ru	1.3	NA	41.9	8.0	1.64	0.8	5.3	1.3

Note: NA, not available

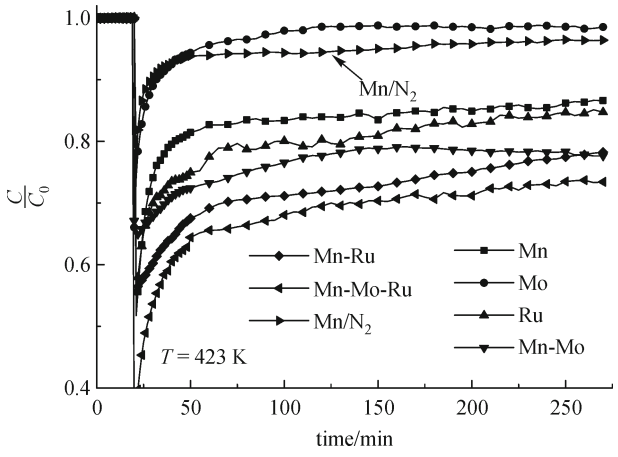

Fig. 3 Adsorption curves of Hg^0 with catalysts doped with various transition metals, at 423 K, [HCl] = [SO_2] = 0, C_0 was about 24 ppbv, air was used as carrier gas except Mn/N_2 with N_2 as carrier gas

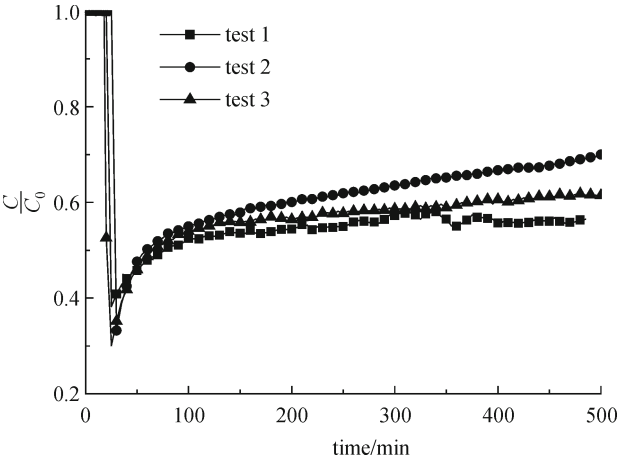

Fig. 5 Influence of Cl_2 on Hg^0 removal with Mn-Mo-Ru catalyst, at 423 K, air as carrier gas, C_0 was about 23 ppbv, [Cl_2] = 0.5 ppmv, [SO_2] = [HCl] = 0

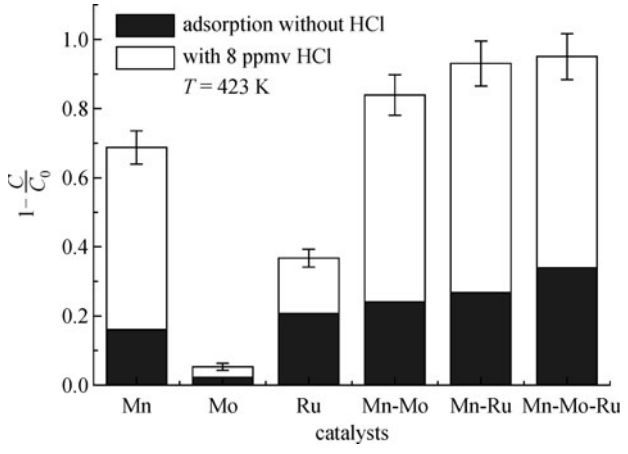

Fig. 4 Removal efficiencies of Hg^0 with the catalysts doped with various transition metals, at 423 K, [HCl] = 8 ppmv, [SO_2] = 0, C_0 was about 23.5 ppbv, and air was used as carrier gas

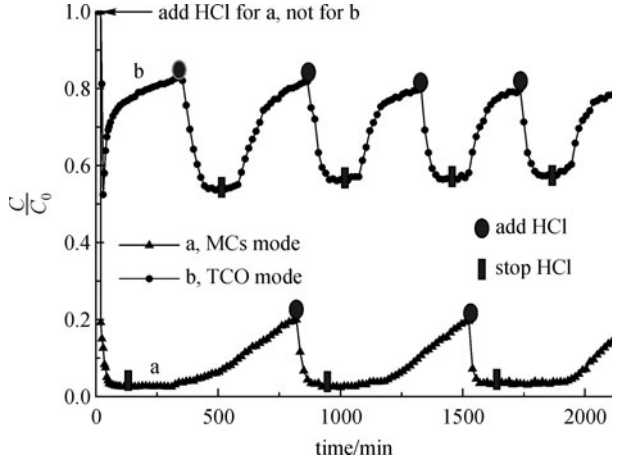

Fig. 6 Influence on Hg^0 removal with intermittent injection of HCl in the MCs and the TCO mode, [HCl] = 8 ppmv, C_0 was about 23 ppbv, air as carrier gas, [SO_2] = 0, Mn-Mo-Ru as catalyst, T = 423 K

membrane material loaded with transition metals had obvious retainability for HCl, which could keep higher removal efficiencies for Hg^0 in the MCs mode after the injection of HCl was stopped.

The measurement result of escaped HCl showed that the concentration of escaped HCl was less than 1 mg·m^{-3}. It indicates that most of injected HCl were retained in the membrane material. Part of the retained HCl was converted to Cl_2. Therefore, the injection of HCl could be intermittently operated in practice (e.g., every 3–4 h) in the MCs, so that the utilization of HCl was higher and its escape into flue gas could be minimized.

Moreover, the analysis of mercury speciation showed that the proportion of mercury (II) chloride on the surface of the catalysts in the TCO and MCs were 54% and 91%, respectively. It further validated the effect of the mode of mass delivery on the Deacon reaction in the MCs.

3.5 Influence of SO_2

Previous studies demonstrated that SO_2 had an obvious interference with the removal of Hg^0 in coal-fired flue gas [3,5,12]. Because the concentration of SO_2 in the test was much higher than that of Cl_2 or $[Cl]^*$, the inhibitory effect of SO_2 against Hg^0 removal was possibly due to the irreversible reaction between adsorbed $SO_{2(ad)}$ and Cl_2 or $[Cl]^*$ [18,22]. The decrease of active species of chlorine caused the decline of the combination of $Hg_{(ad)}$ and $[Cl]^*$. Simultaneously, $HgSO_4$ could form in the presence of SO_2 and was too tightly adsorbed on the surface of the catalysts

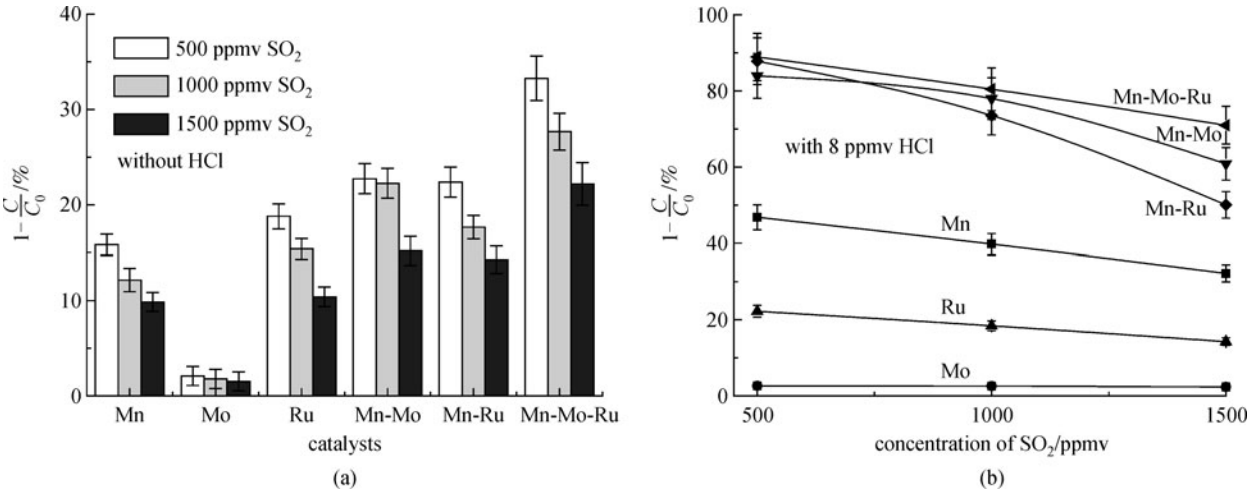

Fig. 7 Influence of SO_2 on the removal for Hg^0, C_0 was about 23 ppbv, air as carrier gas, T = 423 K

to escape along with flue gas, which hampered the adsorption of the catalysts for Hg^0, resulting in the decline of Hg^0 removal. Consequently, a high sulfur–chlorine ratio inhibited the formation of Cl_2 or $HgCl_2$.

To understand the performance of the MCs at test conditions, the inhibition of SO_2 against the removal of Hg^0 was investigated with various concentration of SO_2 at 423 K, and the results were shown in Fig. 7. As shown in Fig. 7(a), the inhibition against Hg^0 removal was obvious when SO_2 was introduced, and the removal efficiency of elemental mercury by Mn-Mo-Ru catalyst declined from 40% to 29%. The removal efficiency of Hg^0 decreased by 14% from 95% with 8 ppmv HCl to 81% after 1000 ppmv SO_2 was used, as shown in Fig. 7(b). It demonstrates that the presence of SO_2 showed an obvious interference with Hg^0 removal by Mn-Mo-Ru catalyst in the presence of HCl.

3.6 Influence of NO

It has been reported that NO showed an obvious influence on Hg^0 oxidation by gas-phase reactions [20,23,24]. However, much research have manifested that its effect was insignificant on the heterogeneous catalytic reaction [2,25–27]. Generally, the concentration of NO in flue gas ranges 100–1000 ppmv [28]. Since the De-NO_x utilities are usually installed upstream of the flue gas equipments, including the MCs, the inlet concentration of NO in the MCs would be low. The effects of NO on elemental mercury removal were investigated with the air as the carrier gas. The results were shown in Fig. 8.

Compared column a with column b in Fig. 8, it can be seen that the influence of NO on Hg^0 removal was neglectable in the absence of HCl, even if the concentration of SO_2 reached 1500 ppmv. However, the Hg^0 removal efficiency slightly increased with the increase of NO in the presence of HCl, even if the concentration of SO_2 reached 1500 ppmv (columns c and d in Fig. 8). Compared with the influence of SO_2 on the removal of Hg^0, Fig. 8 shows that the addition of NO had a weak promotion on sulfur-tolerance (list in Table 2). However, the promoted influence on Hg^0 removal was neglectable [2,26].

During elemental mercury oxidization over metal catalysts, $[Cl]^*$ (or $HCl_{(ad)}$) may react with $NO_{(ad)}$ to form unstable $[NOCl]_{(ad)}$ [29]. Then $Hg_{(ad)}$ reacted with $[NOCl]_{(ad)}$ to form $HgCl_{(ad)}$, resulting in the conversion of Hg^0 to oxidized Hg. This mechanism was similar to that of SO_2.

3.7 Reducibility

H_2-TPR profiles of Mn and Mn-Mo-Ru catalysts are illustrated in Fig. 9. Figure 9(a) shows two H_2-consump-

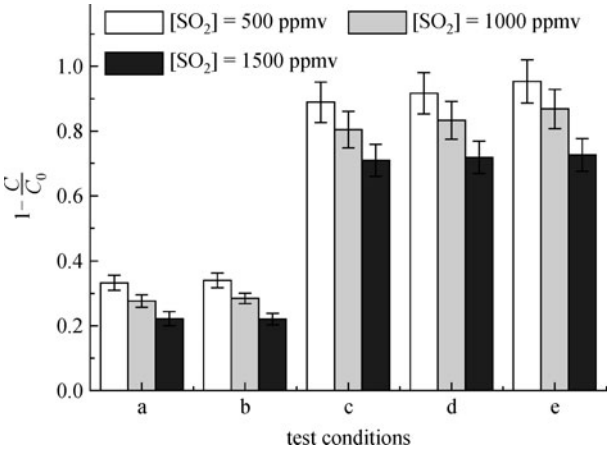

Fig. 8 Influence on Hg^0 removal with various concentration of SO_2 (a, [HCl] = [NO] = 0; b, [HCl] = 0, [NO] = 100 ppmv; c, [HCl] = 8 ppmv, [NO] = 0; d, [HCl] = 8 ppmv, [NO] = 100 ppmv; and e, [HCl] = 8 ppmv, [NO] = 200 ppmv. Air was used as carrier gas, Mn-Mo-Ru as catalyst, T = 423 K, C_0 was about 23.2 ppbv)

Table 2 Influence of NO on sulfur-tolerance with Mn-Mo-Ru catalyst and 8 ppmv HCl

concentration of SO_2	removal efficiencies of Hg^0/%		
	[NO] = 0	[NO] = 100 ppmv	[NO] = 200 ppmv
500	88.9	91.7	95.3
1000	80.5	83.3	86.8
1500	70.9	71.9	72.6

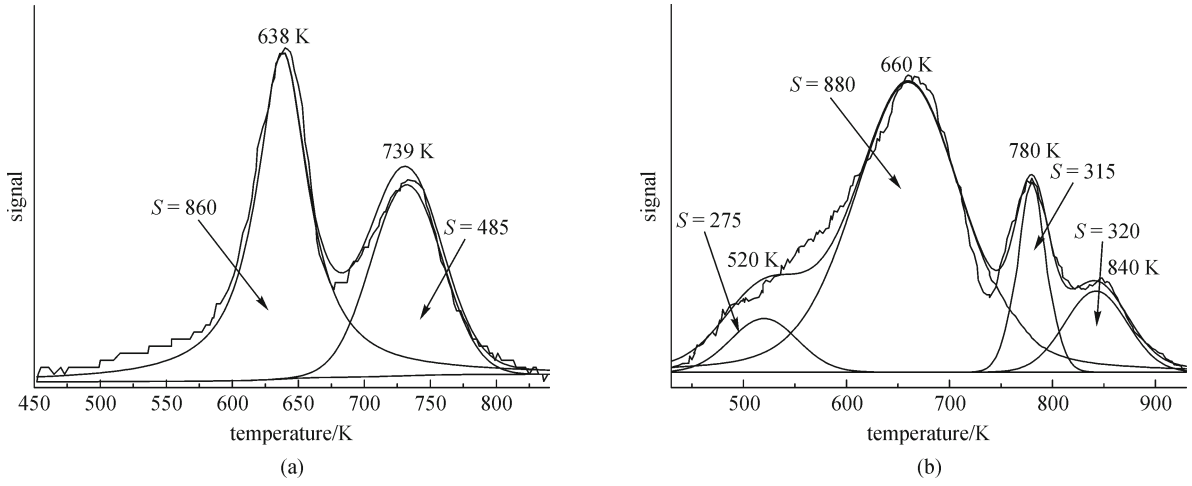

Fig. 9 TPR profiles and the peak results (a) Mn catalyst, (b) Mn-Mo-Ru catalyst (dash is fitted results), symbol *S* denotes the area of corresponding reduction peak

Table 3 Results of H2-TPR profiles of Mn and Mn-Mo-Ru catalysts

catalysts	maximum reduction temperature/K				ratio of Mn^{4+}/Mn^{3+} of TPR data	ratio of Mn^{4+}/Mn^{3+} of XPS data
	$MnO_2 \rightarrow Mn_2O_3$	$Mn_2O_3 \rightarrow Mn_3O_4$	$MoO_3 \rightarrow MoO_2$	$RuO_2 \rightarrow Ru$		
Mn	638	739	–	–	1.77	1.63
Mn-Mo-Ru	660	780	840	520	2.79	2.52

tion peaks for Mn catalyst, which corresponded to the two reduction steps of MnO_x. The peak at 638 K was assigned to the reduction of MnO_2 to Mn_2O_3, and the peak at 739 K was attributed to the reduction of Mn_2O_3 to Mn_3O_4 [30,31]. As shown in Fig. 9(b), H_2-TPR profile of Mn-Mo-Ru catalyst revealed four peaks. The peak at 840 K may be ascribed to the reduction of MoO_3 to MoO_2 [32].

Based on the present test and previous results [33], $RuCl_3$ can be oxidized on the surface of the catalysts by the air at room temperature. Moreover, the color variation of the catalysts indicated the substitution of chloride into an oxide. Thus, the peak at 520 K can be attributed to the reduction of RuO_2 to Ru [33,34].

Compared with that in Fig. 9(a), H_2-consumption area of the reduction of MnO_2 to Mn_2O_3 (named $area_{MnO_2}$) slightly increased, although the peak intensity declined slightly (shown in Fig. 9(b)). H_2-consumption area of the reduction of Mn_2O_3 to Mn_3O_4 (named $area_{Mn_2O_3}$) decreased clearly after the incorporation of other metals. Because H_2-consumption area approximately represents the reducible amount of Mn, the variation of the ratio of Mn^{4+} to Mn^{3+} on the surface of catalysts can be got from the $area_{MnO_2}$ and $area_{Mn_2O_3}$ (shown in Fig. 9). As shown in Table 3, the ratio of Mn^{4+} to Mn^{3+} increased from 1.77 to 2.79.

3.8 XPS

Surface information on the membrane catalyst was analyzed by XPS, and the XPS spectra over the spectral regions of Mn 2p, Mo 3d, O 1s and S 2p were evaluated (shown in Fig. 10). By comparison with the Mn 2p XPS spectrum database of the National Institute of Standards and Technology (NIST) [35], Mn on the catalysts were determined to be mainly present in the states of Mn (IV) and Mn (III). Moreover, the ratio of Mn (IV) to Mn (III) increased greatly after catalytic oxidation under air (shown in Fig. 10(b)). This result was consistent with the results of TPR profile (shown in Table 3). It suggests that the reduced Mn (IV) could be completely regenerated under air.

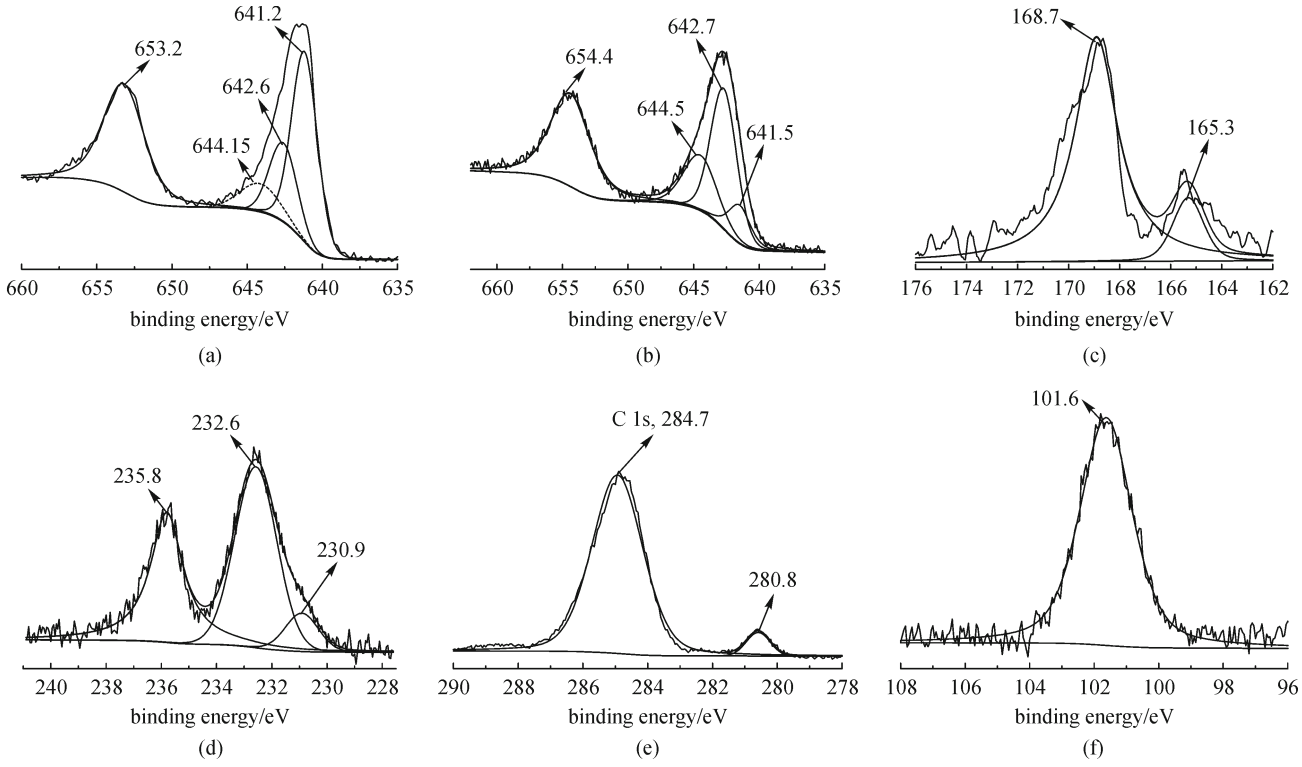

Fig. 10 XPS spectroscopes of Mn 2p, Mo 3d, Ru 3d, Hg 4f and S 2P (dash is fitted results) (a) Mn 2p, N_2 as carrier gas; (b) Mn 2p, air as carrier gas; (c) S 2p, air as carrier gas; (d) Mo 3d, air as carrier gas; (e) Ru 3d, air as carrier gas; (f) Hg 4f, air as carrier gas. Mn-Mo-Ru catalyst was used, C_0 was about 15–20 ppbv, [HCl] = 8 ppmv, [SO_2] = 1000 ppmv

The Mo 3d peaks centered at 232.5, 235.8, and 230.8 eV, were attributed to Mo (VI) and Mo (IV), respectively. The BEs of ruthenium and oxygen (Ru $3d_{5/2}$ at 280.7 eV, and O 1s at 529.7 eV) were the characteristic of polycrystalline RuO_2 [36]. The result was identical in the fresh and used catalysts and consistent with previous studies [33].

On the basis of the result of S 2p XPS (Fig. 10(c)) and combined with the spectra of Hg 4f (Fig. 10(f)), it can be confirmed that Hg specie was assigned to $HgSO_4$ (BE 168.7 eV) after HCl was used by the NIST XPS database and pervious literatures [35].

3.9 Mass balance

To validate the removal efficiencies of the MCs for Hg^0 removal, the mass balance of mercury was carried out using the OHM method. The operation parameters were similar to that of Hg^0 conversion in the presence of only HCl in this study. The input Hg^0 concentration was continuously measured for at least two days prior to each adsorption experiment to ensure a constant Hg^0 input concentration. Three replicate tests were conducted to analyze the speciation of Hg after HCl was used, and the results were shown in Fig. 11.

As shown in Fig. 11, the mass balance of three replicate tests was all in a reasonably acceptable value of 93%–103% (mean value of 34 μg). The removal efficiency of Hg was determined by the amount of Hg^{2+}-ad and Hg^{2+}-out.

As shown in Fig. 11, the mean percentage of Hg^{2+}-ad and Hg^{2+}-out in three tests was 14% and 78%, respectively, with the mean removal efficiency of 93.4%, which further validated that the MCs had higher conversion efficiency for Hg^0 at low temperature. It indicates that most of adsorbed mercury on the surface of the catalysts was

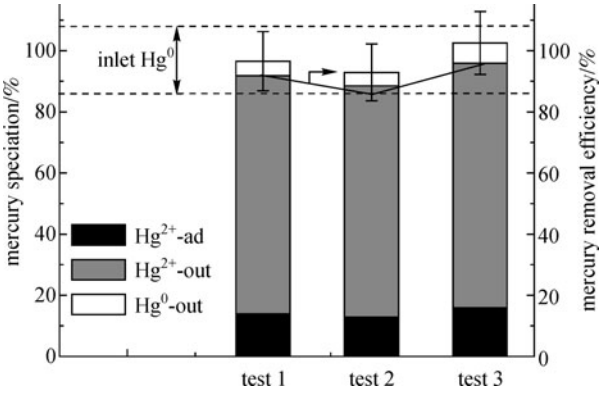

Fig. 11 Mercury speciation results of three replicate tests, Mn-Mo-Ru was used as catalyst, C_0 was about 23 ppbv, [HCl] = 8 ppmv, [SO_2] = 0, T = 423 K

oxidized mercury in the presence of HCl, with the mass balance of 92%±4%. These results were consistent with the conversion analysis of Hg^0.

4 Conclusions

The conversion of Hg^0 to Hg^{2+} using the membrane catalytic technology at 423 K was investigated. The higher conversion of Hg^0 was realized over the membrane material loaded with transition metals of Mn, Mo, and Ru. The test results show that the removal efficiencies of Hg^0 over Mn-Mo-Ru catalyst reached 95% in the presence of 8 ppmv HCl. The influence of NO and SO_2 on Hg^0 removal was insignificant. The mass balance analysis of Hg indicated that most of adsorbed mercury on the surface of the catalysts were oxidized mercury in the presence of HCl. The transition metals of Mn, Mo, and Ru played a key role during the process of removal and conversion of Hg^0. Moreover, Mn-Mo-Ru catalyst had excellent performance for the conversion of the Deacon reaction.

Compared with the TCO mode, the membrane catalytic technology appears to be a potential and novel mode for the conversion of Hg^0 in coal-fired flue gas.

Acknowledgements This work was supported by the High-Tech Research & Development Program of China (No. 2007AA06Z340) and the National Natural Science Foundation of China (Grant No. 21077073).

References

1. Liu Y, Kelly D J A, Yang H Q, Lin C C H, Kuznicki S M, Xu Z G. Novel regenerable sorbent for mercury capture from flue gases of coal-fired power plant. Environmental Science & Technology, 2008, 42(16): 6205–6210
2. Li Y, Murphy P D, Wu C Y, Powers K W, Bonzongo J C J. Development of silica/vanadia/titania catalysts for removal of elemental mercury from coal-combustion flue gas. Environmental Science & Technology, 2008, 42(14): 5304–5309
3. Guo Y F, Yan N Q, Yang S J, Qu Z, Wu Z B, Liu Y, Liu P, Jia J P. Conversion of elemental mercury with a novel membrane delivery catalytic oxidation system (MDCOs). Environmental Science & Technology, 2011, 45(2): 706–711
4. Niksa S, Fujiwara N. The impact of wet flue gas desulfurization scrubbing on mercury emissions from coal-fired power stations. Journal of the Air & Waste Management Association, 2005, 55(7): 970–977
5. Kim M H, Ham S W, Lee J B. Oxidation of gaseous elemental mercury by hydrochloric acid over $CuCl_2/TiO_2$-based catalysts in SCR process. Applied Catalysis B: Environmental, 2010, 99(1–2): 272–278
6. Lee W J, Bae G N. Removal of elemental mercury (Hg(O)) by nanosized V_2O_5/TiO_2 catalysts. Environmental Science & Technology, 2009, 43(5): 1522–1527
7. He S, Zhou J, Zhu Y, Luo Z, Ni M, Cen K. Mercury oxidation over a vanadia-based selective catalytic reduction catalyst. Energy & Fuels, 2009, 23(1): 253–259
8. Kamata H, Ueno S, Sato N, Naito T. Mercury oxidation by hydrochloric acid over TiO_2 supported metal oxide catalysts in coal combustion flue gas. Fuel Processing Technology, 2009, 90(7–8): 947–951
9. Straube S, Hahn T, Koeser H. Adsorption and oxidation of mercury in tail-end SCR-DeNO_x plants—bench scale investigations and speciation experiments. Applied Catalysis B: Environmental, 2008, 79(3): 286–295
10. Liu F D, He H, Ding Y, Zhang C B. Effect of manganese substitution on the structure and activity of iron titanate catalyst for the selective catalytic reduction of NO with NH_3. Applied Catalysis B: Environmental, 2009, 93(1–2): 194–204
11. Jing G H, Li J H, Yang D, Hao J M. Promotional mechanism of tungstation on selective catalytic reduction of NO_x by methane over $In/WO_3/ZrO_2$. Applied Catalysis B: Environmental, 2009, 91(1–2): 123–134
12. Presto A A, Granite E J. Noble metal catalysts for mercury oxidation in utility flue gas gold, palladium and platinum formulations. Platinum Metals Review, 2008, 52(3): 144–154
13. Poulston S, Granite E J, Pennline H W, Myers C R, Stanko D P, Hamilton H, Rowsell L, Smith A W J, Ilkenhans T, Chu W. Metal sorbents for high temperature mercury capture from fuel gas. Fuel, 2007, 86(14): 2201–2203
14. Li J F, Yan N Q, Qu Z, Qiao S H, Yang S J, Guo Y F, Liu P, Jia J P. Catalytic oxidation of elemental mercury over the modified catalyst Mn/alpha-Al_2O_3 at lower temperatures. Environmental Science & Technology, 2010, 44(1): 426–431
15. Qiao S H, Chen J, Li J F, Qu Z, Liu P, Yan N Q, Jia J P. Adsorption and catalytic oxidation of gaseous elemental mercury in flue gas over MnO_x/alumina. Industrial & Engineering Chemistry Research, 2009, 48(7): 3317–3322
16. Zhao Y C, Zhang J Y, Liu J, Diaz-Somoano M, Martinez-Tarazona M R, Zheng C G. Study on mechanism of mercury oxidation by fly ash from coal combustion. Chinese Science Bulletin, 2010, 55(2): 163–167
17. Li J H, Liang X, Xu S C, Hao J M. Catalytic performance of manganese cobalt oxides on methane combustion at low temperature. Applied Catalysis B: Environmental, 2009, 90(1–2): 307–312
18. Galbreath K C, Zygarlicke C J. Mercury transformations in coal combustion flue gas. Fuel Processing Technology, 2000, 65–66: 289–310
19. Pan H Y, Minet R G, Benson S W, Tsotsis T T. Process for converting hydrogen chloride to chlorine. Industrial & Engineering Chemistry Research, 1994, 33(12): 2996–3003
20. Li Y, Murphy P, Wu C Y. Removal of elemental mercury from simulated coal-combustion flue gas using a SiO_2-TiO_2 nanocomposite. Fuel Processing Technology, 2008, 89(6): 567–573
21. Cao Y, Chen B, Wu J, Cui H, Smith J, Chen C K, Chu P, Pan W P. Study of mercury oxidation by a selective catalytic reduction catalyst in a pilot-scale slipstream reactor at a utility boiler burning bituminous coal. Energy & Fuels, 2007, 21(1): 145–156
22. Lindbauer R L, Wurst F, Prey T. Combustion dioxin suppression in municipal solid-waste incineration with sulfur additives. Chemosphere, 1992, 25(7–10): 1409–1414
23. Norton G A, Yang H Q, Brown R C, Laudal D L, Dunham G E,

Erjavec J. Heterogeneous oxidation of mercury in simulated post combustion conditions. Fuel, 2003, 82(2): 107–116

24. Zhao Y X, Mann M D, Olson E S, Pavlish J H, Dunham G E. Effects of sulfur dioxide and nitric oxide on mercury oxidation and reduction under homogeneous conditions. Journal of the Air & Waste Management Association (1995), 2006, 56(5): 628–635
25. Krishnakumar B, Helble J J. Understanding mercury transformations in coal-fired power plants: evaluation of homogeneous Hg oxidation mechanisms. Environmental Science & Technology, 2007, 41(22): 7870–7875
26. Niksa S, Helble J J, Fujiwara N. Kinetic modeling of homogeneous mercury oxidation: the importance of NO and H_2O in predicting oxidation in coal-derived systems. Environmental Science & Technology, 2001, 35(18): 3701–3706
27. Agarwal H, Stenger H G, Wu S, Fan Z. Effects of H_2O, SO_2, and NO on homogeneous Hg oxidation by Cl_2. Energy & Fuels, 2006, 20(3): 1068–1075
28. Hall B, Schager P, Lindqvist O. Chemical reactions of mercury on combustion flue gases. Water, Air, and Soil Pollution, 1991, 56(1): 3–14
29. Hrdlicka J A, Seames W S, Mann M D, Muggli D S, Horabik C A. Mercury oxidation in flue gas using gold and palladium catalysts on fabric filters. Environmental Science & Technology, 2008, 42(17): 6677–6682
30. Álvarez-Galván M C, de la Peña O'Shea V A, Fierro J L G, Arias P L. Alumina-supported manganese- and manganese-palladium oxide catalysts for VOCs combustion. Catalysis Communications, 2003, 4 (5): 223–228
31. Ji L, Sreekanth P M, Smirniotis P G, Thiel S W, Pinto N G. Manganese oxide/titania materials for removal of NO_x and elemental mercury from flue gas. Energy & Fuels, 2008, 22(4): 2299–2306
32. Liu H, Xu Y. H_2-TPR study on Mo/HZSM-5 catalyst for CH_4 dehydroaromatization. Chinese Journal of Catalysis, 2006, 27(4): 319–323
33. Mazzieri V, Coloma-Pascual F, Arcoya A, L'Argentière P, Fígoli N S. XPS, FTIR and TPR characterization of Ru/Al_2O_3 catalysts. Applied Surface Science, 2003, 210(3–4): 222–230
34. Bianchi C L. TPR and XPS investigations of Co/Al_2O_3 catalysts promoted with Ru, Ir and Pt. Catalysis Letters, 2001, 76(3–4): 155–159
35. NIST XPS Database. http://srdata.nist.gov/xps/.accessed August, 2007
36. López N, Gómez-Segura J, Marín R P, Pérez-Ramírez J. Mechanism of HCl oxidation (Deacon process) over RuO_2. Journal of Catalysis, 2008, 255(1): 29–39